

Lightweight Self-Supervised Detection of Fundamental Frequency and Accurate Probability of Voicing in Monophonic Music

Venkat Suprabath Bitra¹ ^a and Homayoon Beigi² ^b

¹Dept. of Computer Science, Columbia University, New York, US

²Dept. of Mechanical Engineering and Dept. of Electrical Engineering, Columbia University, and Recognition Technologies, Inc., New York, US
venkat.s.bitra@columbia.edu, homayoon.beigi@columbia.edu

Accepted for publication at ICPRAM 2026, March 2-4, 2026, Marbella, Spain

Keywords:

self-supervised pitch detection, unsupervised pitch detection, fundamental frequency, pitch estimation, resonance, musical timbre transfer, probability of voicing, music synthesis, music analysis, CQT, constant Q transform, DDSP, shift cross-entropy loss, musical instrument modeling, ResNeXt neural network, music information retrieval, MIR

Abstract:

Reliable fundamental frequency (F_0) and voicing estimation is essential for neural synthesis, yet many pitch extractors depend on large labeled corpora and degrade under realistic recording artifacts. We propose a lightweight, fully self-supervised framework for joint F_0 estimation and voicing inference, designed for rapid single-instrument training from limited audio. Using transposition-equivariant learning on CQT features, we introduce an EM-style iterative reweighting scheme that uses Shift Cross-Entropy (SCE) consistency as a reliability signal to suppress uninformative noisy/unvoiced frames. The resulting weights provide confidence scores that enable pseudo-labeling for a separate lightweight voicing classifier without manual annotations. Trained on MedleyDB and evaluated on MDB-stem-synth ground truth, our method achieves competitive cross-corpus performance (RPA 95.84, RCA 96.24) and demonstrates cross-instrument generalization.

1 INTRODUCTION

Estimating the fundamental frequency (F_0) and whether a signal is voiced are core primitives for speech and music analysis and they underpin a wide range of downstream systems in Music Information Retrieval (MIR), audio editing, and neural synthesis (Beigi, 2011; Yost, 2009). Classical pitch trackers such as YIN (de Cheveigné and Kawahara, 2002), RAPT (Talkin, 1995), and pYIN (Mauch and Dixon, 2014) exploit periodicity and heuristics that work well in controlled conditions, but become brittle under realistic acoustic artifacts and domain shift.

Deep learning approaches (e.g., CREPE (Kim et al., 2018)) have substantially improved accuracy on benchmark datasets, yet two practical barriers limit their usefulness for rapid,

customized audio pipelines. First, most high-performing models are supervised and therefore rely on large, carefully annotated corpora that are expensive to build and difficult to scale across instruments, recording conditions, and playing techniques. Second, models trained on curated data often generalize poorly when deployed on real recordings with bleeding, reverberation, and background noise (Morrison et al., 2024; Saxena et al., 2024; Geirhos et al., 2020). These barriers are especially problematic for modern synthesis workflows, where feature extractors must be adapted quickly to a target instrument or recording setup.

A motivating example is Differentiable Digital Signal Processing (DDSP) and related neural synthesis systems (Engel et al., 2020a; Hayes et al., 2023). These frameworks can produce high-quality, personalized instruments, but assume reliable F_0 and voicing features. Practi-

^a  <https://orcid.org/0000-0002-9254-2274>

^b  <https://orcid.org/0000-0003-0127-2385>

tioners often aim to build a custom synthesizer from minutes of audio rather than hours, yet many current pitch extractors, supervised or self-supervised, are trained on large corpora and are not designed to converge robustly in low-data, single-instrument settings. This mismatch creates a bottleneck: even if synthesis can be personalized from 10 to 15 minutes of audio, the feature extractor may not be able to.

This paper reframes pitch estimation as a low-data, single-instrument, fast-training problem. Our goal is to learn an F_0 /voicing front-end that can be trained efficiently from a small amount of target audio, while remaining reliable on real recordings. To emphasize realistic acoustics, we focus on MedleyDB (Bittner et al., 2014), which contains genuine multitrack recordings and therefore exhibits bleed, room effects, and non-ideal isolation. This setting is materially different from digitally resynthesized or perfectly separated datasets (e.g., MDB-stem-synth (Salamon et al., 2017)), where unvoiced segments may be near-silent and interference is minimal. Robustness in MedleyDB is critical if the extracted features are to serve as dependable signals for synthesis.

To eliminate the need for manual pitch labels and to support rapid adaptation, we adopt self-supervised learning (SSL) with a transposition-equivariant objective inspired by SPICE (Gfeller et al., 2020) and PESTO (Riou et al., 2023). Using a Constant-Q Transform (CQT) representation (Brown, 1991), we train the model to satisfy a simple consistency constraint: if the input audio is pitch-shifted by a known interval, the model’s internal pitch representation must shift by the same amount. This equivariance “pretext task” forces the network to encode pitch structure directly, without supervision, and provides a natural mechanism for learning from small, instrument-specific collections.

Beyond F_0 , we target robust voicing detection under interference. In real recordings, “unvoiced” does not imply silence; it often contains residual energy from bleed and noise. We exploit this reality through the Shift Cross-Entropy (SCE) loss: the equivariant objective is minimized only when the pitch representation is stable and unambiguous, a condition that is strongly correlated with genuinely voiced content. We use this stability signal to construct reliable pseudo-labels and train a dedicated voicing classifier, producing an F_0 /voicing pipeline that is both label-free and resilient to realistic artifacts.

2 CONTRIBUTIONS

- Training exclusively on MedleyDB’s (Bittner et al., 2014) acoustically challenging multitrack recordings to ensure robustness against realistic noise, bleed, and artifacts.
- Two-stage pseudo-labeling method where unsupervised Shift Cross-Entropy loss generates confidence scores for training a lightweight binary voicing classifier without manual labels.
- Rigorous cross-instrument evaluation quantifying timbre-independent pitch generalization by training on single instruments and testing on unseen instruments.

3 METHODS

We build on the self-supervised, transposition-equivariant learning paradigm of PESTO to estimate both fundamental frequency (F_0) and voicing from isolated monophonic instrument stems. Our method is tailored to single-instrument, low-data training by (i) a CQT front-end that aligns augmentation with musical transposition, (ii) an efficient ResNeXt1D encoder with a Toeplitz-structured pitch head, and (iii) a two-stage voicing pipeline that converts self-supervised stability signals into pseudo-labels for a lightweight binary classifier. The following subsection details the data, feature extraction, augmentations, architecture, and objectives; the next subsection introduces our EM-based reweighting strategy.

3.1 Dataset and Feature Extraction

3.1.1 Datasets

We train on instrument-specific stems from MedleyDB (Bittner et al., 2014), which contains real multitrack recordings and therefore exhibits realistic interference such as bleed, room reverberation, and recording noise. For evaluation, we use MDB-stem-synth (Salamon et al., 2017), which provides precise, frame-level ground-truth F_0 labels derived from MIDI-controlled synthesis. Both datasets provide pre-separated stems, avoiding the need for source separation during training and testing. A detailed comparison between MedleyDB and MDB-stem-synth is provided in Section 4.1.

3.1.2 Constant-Q Transform (CQT) Input

Each audio clip is converted to a log-magnitude CQT representation. Let a single time frame be $x \in \mathbb{R}^B$ and a training batch be $X \in \mathbb{R}^{N \times B}$, where B is the number of CQT frequency bins and N is the number of sampled frames. We use $f_{\min} = A0 \approx 27.5\text{Hz}$ and 36 bins per octave (i.e., $B_{\text{st}} = 3$ bins per semitone). The transform uses $B = 269$ bins, spanning approximately 7.5 octaves up to $f_{\max} \approx 4.9\text{kHz}$, covering the pitched range through C8 $\approx 4.2\text{kHz}$.

Although the target stems in our experiments predominantly occupy an F_0 range of roughly 200-1200Hz, we retain a wider CQT band to provide headroom for transposition-based self-supervision. With $f_s = 16\text{kHz}$ (Nyquist frequency = 8kHz), content above $\sim 4\text{kHz}$ carries limited harmonic evidence for this F_0 range. It is included primarily to reduce edge effects, i.e., to lower the probability that pitch shifts push the predicted mode to a boundary bin and cause representation collapse.

3.1.3 Transposition Equivariance via CQT Shifts

Self-supervision is defined on pitch-shifted pairs (x, x') extracted from the same underlying audio. A transposition of τ semitones corresponds to a bin shift $\delta = \tau B_{\text{st}}$. We approximate the shifted view by a discrete shift along the CQT frequency axis,

$$x'(b) \approx x(b - \delta),$$

where b indexes CQT bins. The learning objective enforces equivariance: the predicted pitch distribution for x' should match the prediction for x shifted by δ bins. In practice, shifts are applied with boundary-safe padding (rather than wrap-around) to avoid introducing non-physical energy at the frequency limits.

3.1.4 Pitch-Invariant Augmentations

To encourage invariance to loudness and background perturbations, we apply independent augmentations to each view. Let x denote the log-magnitude CQT frame and $m = \exp(x)$ its linear magnitude. Define, $\mathcal{U}(a, b)$ as the uniform distribution on $[a, b]$, and $\mathcal{N}(\mu, \sigma^2)$ as a Gaussian (normal) distribution with mean μ and variance σ^2 .

Random gain. We sample $g \sim \mathcal{U}(0.5, 1.5)$ and apply an additive offset in log space:

$$x \leftarrow x + \log(g).$$

SNR-targeted noise. We sample $\text{SNR}_{\text{dB}} \sim \mathcal{U}(15, 50)$ and compute signal power $P_s = \mathbb{E}[m^2]$ over bins. With $\text{SNR} = 10^{\text{SNR}_{\text{dB}}/10}$, we set $P_n = P_s/\text{SNR}$ and draw $n \sim \mathcal{N}(0, P_n)$:

$$m \leftarrow m + n, \quad x \leftarrow \log(\max(m, \varepsilon)),$$

where ε prevents the logarithm of non-positive values.

3.1.5 Model Architecture

Our network $f_{\theta}(\cdot)$ maps a CQT frame to pitch logits. It consists of a ResNeXt1D encoder followed by a Toeplitz-structured linear classifier (Fig. 1). The encoder comprises a stem convolution and three stages of ResNeXtBlock1D modules with grouped convolutions, enabling multi-scale spectral aggregation with improved parameter efficiency. The pitch head is implemented as a 1D convolution over the frequency axis, imposing a Toeplitz structure that reduces parameters relative to a fully connected classifier. This structure also supports efficient post-hoc calibration: a circular shift of the classifier kernel can correct systematic pitch-bin offsets without retraining.

3.1.6 Training Objectives

Given a batch of paired frames $\{(x_i, x'_i)\}_{i=1}^N$ and corresponding logits $y_i = f_{\theta}(x_i)$ and $y'_i = f_{\theta}(x'_i)$, we define $p_i = \text{softmax}(y_i)$ and $p'_i = \text{softmax}(y'_i)$. We use a weighted sum of three loss terms:

$$\mathcal{L}_{\text{total}} = \frac{1}{N} \sum_{i=1}^N w_i \left(\mathcal{L}_{\text{equiv},i} + \mathcal{L}_{\text{invar},i} + \mathcal{L}_{\text{sce},i} \right)$$

where w_i are sample weights produced by our iterative reweighting scheme (described in the next subsection).

3.2 Iterative Re-weighting using Expectation-Maximization

3.2.1 Intuition

SCE enforces a self-consistency constraint under pitch transposition: if a frame contains a coherent harmonic structure, then the predicted pitch distribution on a transposed view should match a shifted version of the prediction on the original view. Voiced frames approximately satisfy

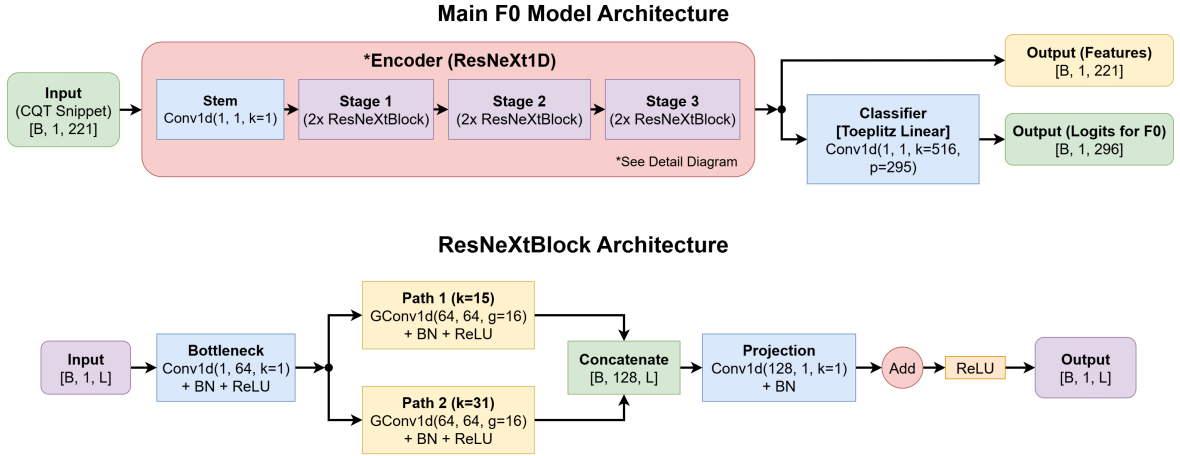


Figure 1: Model architecture. ResNeXt1D encoder over CQT frames followed by a Toeplitz linear classifier (implemented as a 1D convolution) producing pitch logits.

this constraint, yielding aligned targets and low-variance gradients that sharpen the pitch peak. Unvoiced frames (noise, bleed, reverb tails) do not transform into a consistent pitched pattern under transposition, so SCE produces inconsistent targets and high-variance gradients. In low-data regimes, once voiced frames are fit, their SCE becomes small and optimization can become dominated by these uninformative unvoiced gradients. Our EM-style reweighting prevents this by down-weighting frames whose SCE indicates unreliable transposition structure.

3.2.2 Algorithm (EM-style iterative reweighting)

Training alternates between weight estimation (E-step) and weighted optimization (M-step). Let $\mathcal{D} = \{X_i\}_{i=1}^M$ be the training set and initialize $w_i \leftarrow 1$. We update weights every $K = 5$ epochs.

Initialization. Train f_θ for K epochs with $w_i = 1$.

E-step (weight update). At epoch index e (multiple of K), compute $\mathcal{L}_{sce,i}$ for all frames under the current model. Normalize within the pass:

$$\hat{\mathcal{L}}_{sce,i} = \frac{\mathcal{L}_{sce,i} - \min_j \mathcal{L}_{sce,j}}{\max_j \mathcal{L}_{sce,j} - \min_j \mathcal{L}_{sce,j} + \epsilon} \in [0, 1].$$

Define an epoch-dependent annealing factor

$$\lambda(e) = \exp\left(\frac{e^{1.25}}{1000}\right) - 1,$$

and update weights by

$$\Delta w_i = \lambda(e) \hat{\mathcal{L}}_{sce,i} \quad w_i \leftarrow \max(0, w_i - \Delta w_i).$$

Thus, frames with larger SCE are progressively down-weighted as training advances.

M-step (weighted optimization). For the next K epochs, update θ by minimizing the weighted objective. Repeat the E-step and M-step until convergence.

3.2.3 Why reweighting suppresses bad gradients

Let $X \in \mathbb{R}^B$ be a CQT frame and $y = f_\theta(X) \in \mathbb{R}^K$ be the model’s output logits over K pitch bins. Let X' be its transposed view with $y' = f_\theta(X')$. Define $p = \text{softmax}(y)$ and $p' = \text{softmax}(y')$. Let $\text{roll}(y, \delta)$ denote a circular shift by δ bins (pitch transposition in log-frequency space). The Shift Cross-Entropy (SCE) loss compares predictions on an original frame X and its pitch-shifted version X' :

$$\mathcal{L}_{sce} = \frac{1}{2} (\text{CE}(y', \text{roll}(p, \delta)) + \text{CE}(y, \text{roll}(p', -\delta)))$$

where $y = f_\theta(X)$ and $y' = f_\theta(X')$. The gradient of cross-entropy with respect to logits follows the standard form:

$$\frac{\partial \text{CE}(p, q)}{\partial y} = p - q$$

where $p = \text{softmax}(y)$ and q is the target distribution (treated as fixed).

Clean Silence Encourages Trivial Solutions On synthetic datasets (such as MDB-stem-synth), silent frames are exactly zero: $X = \mathbf{0}$. When the input is zero, the model output becomes time-constant: $y = f_\theta(\mathbf{0})$ produces the same logits for all silent frames. With typical initialization, weight decay, and symmetric training data, the network tends to produce approximately uniform predictions on constant inputs, so:

$$p = \text{softmax}(f_\theta(\mathbf{0})) \approx \mathbf{u}$$

where \mathbf{u} is the uniform distribution:

$$u_k = \frac{1}{K}$$

Since uniform distributions are invariant to circular shifts ($\text{roll}(\mathbf{u}, \delta) = \mathbf{u}$), both the prediction and target become uniform:

$$\frac{\partial \mathcal{L}_{\text{sce}}}{\partial y} \approx \mathbf{u} - \mathbf{u} = \mathbf{0}$$

Consequently, the network learns nothing from silent frames and they produce vanishing gradients. This is benign and not informative.

Real Silence is Noisy and Produces Bad Gradients On real recordings (like MedleyDB), “silent” frames are not actually silent. They contain noise, bleed, and reverb: $X = \epsilon$ (random, nonzero). The deep network f_θ is highly nonlinear and sensitive to input perturbations. Even small noise ϵ can produce significantly different outputs:

$$y = f_\theta(\epsilon), \quad p = \text{softmax}(y)$$

Because the noise varies randomly across frames and over time, p fluctuates unpredictably.

Key Issue For the pitch-shifted version $X' = \text{roll}(X, \delta)$, there is no consistent pitch relationship between $p(X')$ and $\text{roll}(p(X), \delta)$ because: (i) Noise has no harmonic pitch structure to transpose, (ii) Different noise realizations (e.g., different positions in reverb tails, different microphone bleed patterns) do not maintain any pitch correspondence under transposition, and (iii) The deep network f_θ may amplify these inconsistencies through its nonlinear layers.

This makes the SCE target $q = \text{softmax}(\text{roll}(y, \delta))$ itself random and inconsistent with the prediction $p' = \text{softmax}(y')$. The gradient variance becomes:

$$\text{Var} \left[\frac{\partial \mathcal{L}_{\text{sce}}}{\partial y_k} \right] = \text{Var}[p_k - q_k] \approx \text{Var}[p_k] + \text{Var}[q_k]$$

This leads to high-variance noisy gradients, “bad gradients”, on unvoiced frames. The model receives contradictory signals across mini-batches, leading to poor convergence, spurious peaks in low-SNR regions and unstable training.

Solution: EM-Style Reweighting Using SCE We treat voicing as a latent variable and use SCE loss as a reliability signal. Frames with low SCE loss have a consistent pitch structure (voiced), while frames with high SCE loss are noisy/unvoiced. The computed gradients for this weighted loss is given as:

$$\frac{\partial}{\partial \theta} [w_i \cdot \text{CE}(p_i, q_i)] = w_i \cdot (p_i - q_i) \cdot \frac{\partial y_i}{\partial \theta}$$

When $\mathcal{L}_{\text{sce},i}$ is large (noisy frame), $w_i \approx 0$, so the gradient contribution vanishes. This:

1. Preserves strong learning on genuinely voiced frames (stable structure \rightarrow low SCE $\rightarrow w \approx 1$)
2. Suppresses high-variance gradients from noisy/unvoiced frames (unstable structure \rightarrow high SCE $\rightarrow w \approx 0$)

The EM approach turns a liability (noisy real-world silence) into an advantage: the model automatically learns to focus on frames with genuine pitch content while ignoring those dominated by noise.

3.3 Supervised Voicing Classification

After self-supervised training, the network $f(\cdot)$ is frozen and the final sample weights $w_i \in [0, 1]$ are thresholded at θ to produce binary pseudo-labels $v_i^* \in \{0, 1\}$. A lightweight linear classifier is then trained on CQT frames using binary cross-entropy against these pseudo-labels, producing robust voicing predictions without any manual annotation. Architectural details are provided in Appendix.

4 Results and Discussion

4.1 Recordings vs. Resynthesized

Figure 2 contrasts CQT magnitude spectrograms from MedleyDB (real multitrack recordings) and MDB-stem-synth (algorithmic resynthesis) over comparable musical segments. The two corpora differ in ways that directly affect both F_0 tracking and voicing.

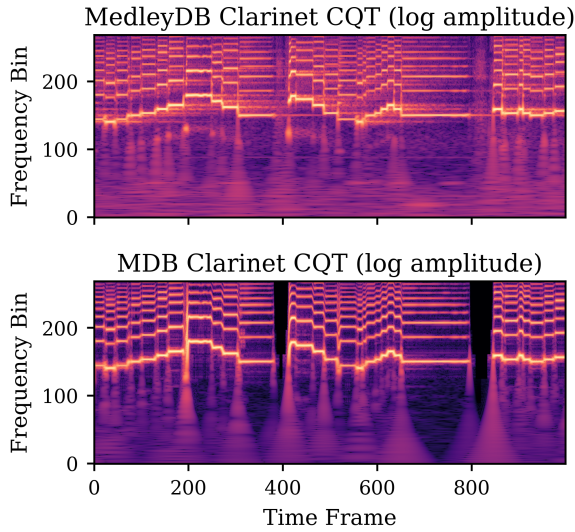


Figure 2: Acoustic comparison: MedleyDB vs. MDB-stem-synth. (Top) MedleyDB recordings show broader partials, modulation sidebands, and exponential decay tails from room acoustics. (Bottom) MDB-stem-synth exhibits narrow harmonic tracks with abrupt terminations and exact silence (black regions). Real recordings retain residual energy from bleed and reverb where synthetic stems are perfectly zero.

MDB-stem-synth exhibits clean harmonic tracks with narrow partial bandwidth and abrupt note offsets, often producing perfectly silent gaps (exact zeros) between notes. In contrast, MedleyDB contains physically plausible decay tails shaped by instrument dynamics, microphone placement, and room acoustics. Real performances also include frequency modulation (vibrato) and amplitude modulation (tremolo), which broaden harmonics and introduce modulation sidebands, visible as wider ridges around the harmonic ladder.

Finally, MedleyDB includes residual room reflections and inter-track bleed that lift the spectral floor and introduce weak cross-harmonic artifacts. These effects are absent in MDB-stem-synth, where “unvoiced” regions are truly anechoic. This discrepancy helps explain why models optimized on resynthesized corpora can degrade on real audio: they are never forced to handle bleed-induced low-SNR frames, realistic decays, or modulation spread. Training exclusively on MedleyDB therefore targets the operating regime required by real-world synthesis and personalization pipelines.

4.2 Effect of EM Reweighting on MedleyDB

Figure 3 visualizes typical behavior on MedleyDB: the CQT with predicted \hat{F}_0 (top), learned sample weights w (middle), and derived voicing proxy \hat{v} (bottom). We observe a consistent pattern across diverse recording conditions. During sustained harmonic regions, weights remain high ($w \approx 1$) and stable, and the predicted \hat{F}_0 follows the dominant harmonic ridge. During note releases, reverberant gaps, and ambiguous low-SNR regions, weights drop sharply, preventing the optimizer from overfitting pitch-unreliable frames.

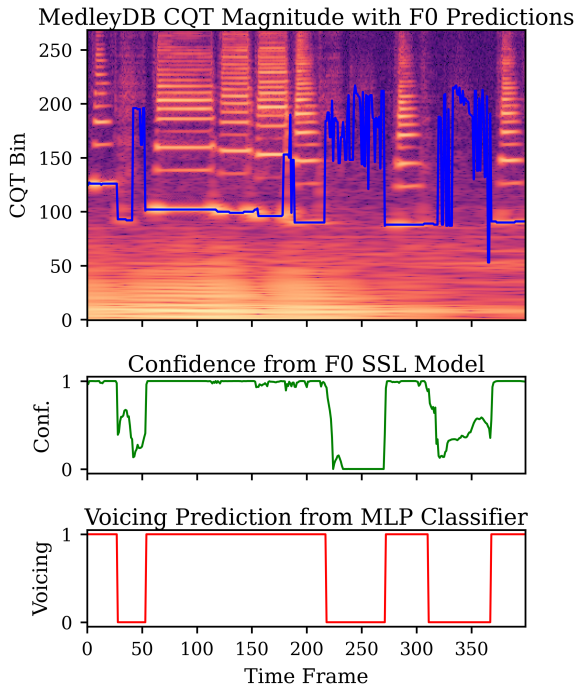


Figure 3: Learned weight behavior on MedleyDB. (Top) CQT spectrogram with predicted F_0 (black). (Middle) EM sample weights w (green) remain high on sustained harmonics and drop during releases and transients. (Bottom) Derived voicing \hat{v} (red) effectively gates voiced segments, automatically distinguishing stable pitch from ambiguous content.

Figure 4 further shows that the learned weights are strongly bimodal (mass concentrated near 0 and 1), indicating that the reweighting naturally separates frames that contain transposition-consistent harmonic structure from frames dominated by noise/bleed. This bimodality also makes the mapping from w to a voicing estimate \hat{v} stable without extensive tuning.

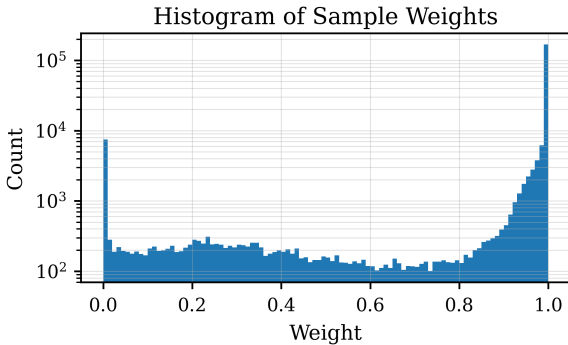


Figure 4: Histogram of EM sample weights on MedleyDB (log-count scale). Clear bimodality: most frames are confidently kept ($w \approx 1$) or down-weighted ($w \approx 0$).

4.3 Cross-Corpus and Cross-Instrument Evaluation

To quantify transfer under realistic acoustics, we train on MedleyDB stems and evaluate on MDB-stem-synth, providing accurate frame-level F_0 labels. We report (i) a compact baseline comparison to contextualize our setting, and (ii) a cross-instrument protocol that trains on a single MedleyDB instrument and tests on unseen instruments in MDB-stem-synth. This isolates timbre generalization while holding evaluation labels fixed and precise. It also reflects the intended use case: rapid, instrument-specific training on real recordings with bleed and reverberation, followed by deployment on cleaner or differently captured audio.

Baseline context. Table 1 summarizes representative supervised (CREPE, DeepF0) and self-supervised (SPICE, DDSP-inv, PESTO) results reported on MDB-stem-synth. In contrast, our primary setting trains on MedleyDB recordings and evaluates on MDB-stem-synth labels, introducing a deliberate domain shift. Despite this mismatch, our method remains competitive: training on MedleyDB and testing on MDB-stem-synth yields RPA = 95.84 and RCA = 96.24, compared to RPA = 96.54 and RCA = 97.55 when trained and tested in-domain on MDB-stem-synth. The small drop (0.70 RPA, 1.31 RCA) indicates that learning under realistic artifacts preserves accuracy on clean evaluation data while improving robustness in the operating regime. For PESTOv2, the values in parentheses denote our CQT-based interpolation of the VQT-reported results, included for a fairer comparison under a single time-frequency representation.

Table 1: Baseline comparison on MDB-stem-synth (RPA/RCA in %). PESTOv2 values in parentheses denote the results for CQT rather than VQT.

Model	RPA	RCA
CREPE (Kim et al., 2018)	96.7	97.0
DeepF0 (Singh et al., 2021)	98.3	98.4
SPICE (Gfeller et al., 2020)	89.1	—
DDSP-inv (Engel et al., 2020b)	88.5	89.6
PESTOv1 (Riou et al., 2023)	94.6	95.0
PESTOv2 (Riou et al., 2025)	94.4	95.0
Ours (MDB → MDB)	96.54	97.55
Ours (Medley → MDB)	95.84	96.24

Cross-instrument transfer. Table 2 reports cross-instrument generalization: each column trains on a single MedleyDB instrument, and each row tests on an unseen MDB-stem-synth instrument. Several transfers exceed 90% RPA on the clean synthetic corpus, consistent with its reduced acoustic complexity (narrower-band partials and exact silences), which makes harmonic structure more separable. Transfer is strongest within the string family (e.g., violin↔cello), reflecting shared excitation mechanisms and overlapping registers. Bass instruments are the hardest targets: averaged across training instruments, electric bass attains the lowest mean RPA ($\approx 68.7\%$) and double bass the next lowest ($\approx 77.2\%$), suggesting that low-frequency dominance and transient-heavy onsets amplify cross-timbre mismatch. Across all conditions, RCA is consistently higher than RPA, indicating that residual errors are dominated by octave confusions rather than arbitrary pitch drift, a favorable failure mode for synthesis and conditioning.

4.4 Short-Segment Additive Resynthesis

For qualitative validation, we drive a simple additive synthesizer using the model’s framewise \hat{F}_0 and voicing weights \hat{v} (details in Appendix). Figure 5 compares CQTs of (a) target MedleyDB audio, (b) synthesized output, and (c) MDB-stem-synth audio.

The synthesized harmonic ladder closely follows the stepwise \hat{F}_0 contour of the target, with transitions occurring at the correct frames, indicating faithful pitch tracking. The voicing gate suppresses ambiguous inter-note regions, producing clear muted spans in the synthesized CQT and removing residual ringing that persists in real recordings (e.g., release tails). Minor triangu-

Table 2: Train on MedleyDB (columns), test on MDB-stem-synth (rows). Metrics are % RPA / RCA.

Instrument Trained →	Clarinet		Cello		Double Bass		Electric Bass		Violin	
Instrument Tested ↓	RPA	RCA	RPA	RCA	RPA	RCA	RPA	RCA	RPA	RCA
Clarinet	94.29	95.37	94.31	95.96	80.61	92.68	96.88	96.98	94.69	95.30
Cello	83.61	86.62	83.29	91.15	96.34	96.65	94.80	95.23	87.96	90.26
Double Bass	54.33	60.45	74.97	82.62	92.88	93.44	88.48	89.68	75.35	81.22
Electric Bass	47.22	60.44	60.68	82.23	89.59	91.36	86.22	88.56	59.69	80.02
Violin	91.50	95.37	91.37	96.65	86.05	91.39	93.48	93.85	93.76	96.07

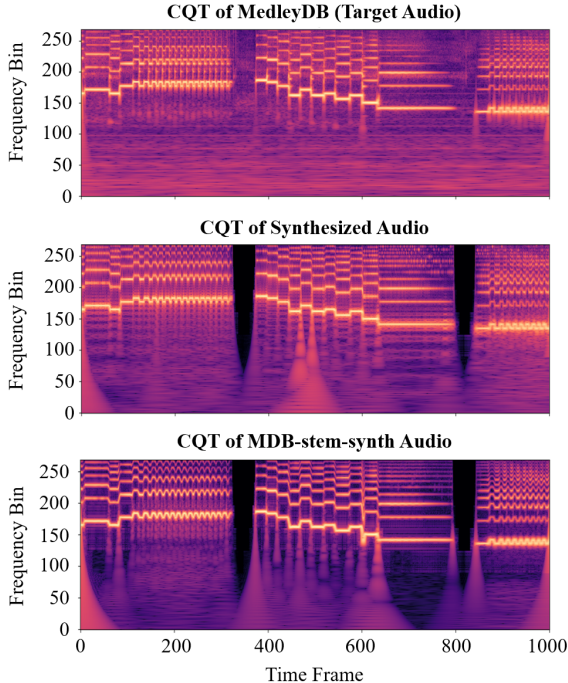


Figure 5: (a) Target audio (CQT). Clear stair-step contours from MedleyDB clarinet with narrow partials and clean inter-note gaps. (b) Synthesized audio (CQT) from \hat{F}_0 and \hat{v} . Harmonic ladders align with the target. The black gaps indicate voicing-controlled muting during predicted unvoiced spans. Low-frequency wedges at the very left/right arise from segment fade-in/out. (c) MDB-stem-synth Synthesis (CQT). Resynthesized audio exhibits narrow, high-contrast harmonic partials with hard on/offsets, exact silences (black gaps), and minimal modulation sidebands compared to real recordings.

lar wedges near segment boundaries arise from overlap-add windowing; they can be reduced with longer fades but are shown here to make gating locations explicit.

5 Conclusion

We presented a lightweight, fully self-supervised framework for joint F_0 estimation and voicing in-

ference from monophonic instrument stems under realistic acoustics. Training exclusively on MedleyDB exposes the model to bleed, reverberation, and low-SNR inter-note regions that commonly break pitch trackers trained on resynthesized data.

Our key contribution is an EM-style iterative reweighting strategy that uses SCE-based transposition consistency as a reliability proxy. Stable harmonic frames retain high weights and drive learning, while unreliable frames are progressively down-weighted, suppressing high-variance gradients. The converged weights serve as confidence scores for pseudo-labeling and training a lightweight binary voicing classifier without manual annotations.

Quantitatively, the method remains competitive under cross-corpus transfer (Medley → MDB: RPA 95.84, RCA 96.24) with only a small gap to in-domain training (MDB → MDB: RPA 96.54, RCA 97.55), and the cross-instrument matrix shows strong within-family transfer with bass instruments remaining the most challenging targets (RCA > RPA, dominated by octave errors). These results support the use of the proposed extractor as a robust front-end for rapid, instrument-specific conditioning in DDSP-style neural synthesis and personalization.

REFERENCES

Beigi, H. (2011). Fundamentals of Speaker Recognition. Springer, New York. ISBN: 978-0-387-77591-3.

Bittner, R. M., Salamon, J., Tierney, M., Mauch, M., Cannam, C., and Bello, J. P. (2014). Medleydb: A multitrack dataset for annotation-intensive mir research. 15th International Society for Music Information Retrieval Conference, Taipei, Taiwan.

Brown, J. C. (1991). Calculation of a constant Q spectral transform. The Journal of the Acoustical Society of America, 89(1):425–434.

de Cheveigné, A. and Kawahara, H. (2002). YIN, a

fundamental frequency estimator for speech and music. *The Journal of the Acoustical Society of America*, 111(4):1917–1930.

Engel, J., Hantrakul, L., Gu, C.-Z., and Roberts, A. (2020a). DDSP: Differentiable digital signal processing. In International Conference on Learning Representations (ICLR).

Engel, J., Hantrakul, L. H., Swavely, R. J., Roberts, A., and Hawthorne, C. G.-M. (2020b). Self-supervised pitch detection by inverse audio synthesis.

Geirhos, R., Jacobsen, J. H., Michaelis, C., Zemel, R., Brendel, W., Bethge, M., and Wichmann, F. A. (2020). Shortcut learning in deep neural networks. *Nature Machine Intelligence*, 2(11):665–673.

Gfeller, B., Frank, C., Roblek, D., Sharifi, M., Tagliasacchi, M., and Velimirovic, M. (2020). SPICE: Self-supervised pitch estimation. *IEEE/ACM Transactions on Audio, Speech, and Language Processing*, 28:1118–1128.

Hayes, B., Shier, J., Fazekas, G., McPherson, A., and Saitis, C. (2023). A review of differentiable digital signal processing for music & speech synthesis. In *Frontiers in Signal Processing*, volume 3.

Huber, P. J. (1964). Robust estimation of a location parameter. *The Annals of Mathematical Statistics*, 35(1):73–101.

Kim, J. W., Salamon, J., Li, P., and Bello, J. P. (2018). CREPE: A convolutional representation for pitch estimation. *ICASSP, IEEE International Conference on Acoustics, Speech and Signal Processing Proceedings*, 2018-April:161–165.

Mauch, M. and Dixon, S. (2014). PYIN: A fundamental frequency estimator using probabilistic threshold distributions. In *2014 IEEE International Conference on Acoustics, Speech and Signal Processing (ICASSP)*, pages 659–663.

Morrison, M., Hsieh, C., Pruyne, N., and Pardo, B. (2024). Cross-domain neural pitch and periodicity estimation. *arXiv preprint arXiv:2301.12258*.

Riou, A., Lattner, S., Hadjeres, G., and Peeters, G. (2023). PESTO: Pitch estimation with self-supervised transposition-equivariant objective. In *Proceedings of the 24th International Society for Music Information Retrieval Conference (ISMIR)*, pages 535–544.

Riou, A., Torres, B., Hayes, B., Lattner, S., Hadjeres, G., Richard, G., and Peeters, G. (2025). Pesto: Real-time pitch estimation with self-supervised transposition-equivariant objective. *Transactions of the International Society for Music Information Retrieval*, 8(1):334–352.

Salamon, J., Bittner, R. M., Bonada, J., Bosch, J. J., Gómez, E., and Bello, J. P. (2017). An analysis/synthesis framework for automatic f0 annotation of multitrack datasets. *Proceedings of the 18th International Society for Music Information Retrieval Conference (ISMIR)*, pages 71–78.

Saxena, K., Kumar, A., Srivastava, P., and Gupta, A. (2024). Interactive singing melody extraction based on active meta-learning for domain adaptation. *arXiv preprint arXiv:2402.07599*.

Singh, S., Wang, R., and Qiu, Y. (2021). Deepf0: End-to-end fundamental frequency estimation for music and speech signals. In *ICASSP 2021 - 2021 IEEE International Conference on Acoustics, Speech and Signal Processing (ICASSP)*, page 61–65. IEEE.

Talkin, D. (1995). A robust algorithm for pitch tracking (RAPT). *Speech Production and Speech Modelling*, pages 495–518.

Yost, W. A. (2009). Pitch perception. *Attention, Perception, and Psychophysics*, 71(8):1701–1715.

APPENDIX

Dataset Details and Statistics

The research in this paper utilizes two distinct datasets: MedleyDB, which consists of real-world multitrack recordings, and MDB-stem-synth, a dataset of clean, resynthesized stems. As noted in the main paper, MedleyDB served as the source for acoustically complex training data (handling bleed, noise, and reverb), while MDB-stem-synth was used for evaluation against a clean, precisely annotated ground truth.

Table 3 provides a detailed statistical comparison of the specific instrument subsets from both datasets used in this study. The comparison highlights the differences in the total number of clips, cumulative audio duration, and average clip length for each instrument.

For the selected instruments, the MedleyDB subset contains a larger clip count (129 vs. 105) and significantly more total audio data (approx. 24.5k seconds vs. 17.9k seconds). This provided a larger and more acoustically diverse corpus for self-supervised training. Notably, the average duration per clip is comparable for some instruments (e.g., violin, electric bass) while diverging on others (e.g., clarinet, double bass), reflecting the different compositions of the two datasets.

Training Objectives

The total loss for a batch of N frames is the average of the per-sample losses, where each component is defined below:

$$\mathcal{L}_{\text{total}} = \frac{1}{N} \sum_{i=1}^N (w_i (\mathcal{L}_{\text{equiv},i} + \mathcal{L}_{\text{invar},i} + \mathcal{L}_{\text{sce},i}))$$

Table 3: Statistical comparison of instrument audio used from MedleyDB (real recordings) and MDB-stem-synth (synthesized stems). Durations are in seconds.

Instrument	MedleyDB (Recordings)			MDB-stem-synth (Synthesized)		
	Clips	Total (s)	Avg. (s)	Clips	Total (s)	Avg. (s)
Clarinet	9	885.39	98.38	8	829.21	103.65
Cello	13	2344.35	180.34	11	1816.80	165.16
Double Bass	17	2919.01	171.71	14	1722.81	123.06
Electric Bass	63	11,398.80	180.93	58	9908.25	170.83
Violin	27	6986.28	258.75	14	3619.81	258.56
Total	129	24533.83	—	105	17896.88	—

This formulation uses the soft weight w_i to ensure that the F_0 -specific equivariance and invariance losses are primarily driven by samples identified as strongly voiced.

Equivariance Loss for F_0 Estimation ($\mathcal{L}_{\text{equiv}}$). To learn F_0 , we enforce pitch equivariance. We define a set of weights $w_k = \alpha^k$ for $k \in \{p_{\min}, \dots, p_{\max}\}$, where α is a constant. If an input X is pitch-shifted by δ bins to produce X' , the corresponding outputs z and z' should satisfy $z' \approx \alpha^\delta z$. The loss is formulated using a symmetric Huber loss (Huber, 1964):

$$\mathcal{L}_{\text{equiv}} = \frac{1}{2} \left(\mathcal{H} \left(\frac{z'}{z} - \alpha^\delta \right) + \mathcal{H} \left(\frac{z}{z'} - \frac{1}{\alpha^\delta} \right) \right)$$

This loss enforces that transposing the input by δ bins produces a corresponding multiplicative shift in the intermediate representation z : specifically, $z' \approx \alpha^\delta z$, where α defines the exponential pitch scale matching the logarithmic CQT structure. The symmetric Huber loss provides robustness against transients and noisy frames while ensuring the model learns pitch intervals as consistent multiplicative factors without requiring labeled data.

Invariance Loss for Timbre Representation ($\mathcal{L}_{\text{invar}}$). While F_0 is equivariant to pitch shifts, the instrumental timbre should be invariant. Given an original output y and the output from a pitch-shifted version y' , the timbre representation should be similar. This is achieved using a symmetric cross-entropy loss (Beigi, 2011):

$$\mathcal{L}_{\text{invar}} = \frac{1}{2} (\text{CE}(y, p') + \text{CE}(y', p))$$

This loss encourages the model to learn pitch-invariant timbre features by enforcing similarity between output logits y and y' from original and pitch-shifted inputs. Since timbre characteristics

such as spectral shape, harmonic decay rates, and formants remain consistent across pitches, the symmetric cross-entropy loss penalizes differences in the predicted distributions. This disentanglement of pitch from timbre is essential for downstream tasks including instrument identification, synthesis control, and timbre transfer, ensuring learned features generalize across different notes from the same instrument.

Shift Cross-Entropy Loss (\mathcal{L}_{sce}). This loss enforces a circular equivariance property and is the key signal for the E-step. If an input is pitch-shifted by δ bins, the output distribution should be circularly shifted by the same amount. Let y be the original output and y' be the transformed output. The loss is (Riou et al., 2023):

$$\mathcal{L}_{\text{sce}} = \frac{1}{2} (\text{CE}(y', \text{roll}(p, \delta)) + \text{CE}(y, \text{roll}(p', -\delta)))$$

This core self-supervised loss enforces circular equivariance: if the input is transposed by δ bins, the output probability distribution should be circularly shifted by the same amount. It compares the predicted distribution from the shifted input with the appropriately rolled version of the original distribution using symmetric cross-entropy. This constraint refines F_0 prediction by ensuring the entire predicted pitch distribution shifts correctly and consistently, encouraging sharp, well-localized probabilities centered on the correct bin. Critically, \mathcal{L}_{sce} also serves as an implicit voicing detector: frames with clear harmonic structure produce sharp distributions that shift predictably, yielding low SCE loss, while noisy or unvoiced frames generate flatter, unstable distributions with high SCE loss. This property enables the E-step of the iterative re-weighting algorithm to automatically identify and down-weight unreliable frames, making F_0 learning robust to real-world noise and artifacts as detailed in .

Voicing Classifier

After the self-supervised representation learning phase is complete, the weights of the network $f(\cdot)$ are frozen. The final set of sample weights, w_i , computed for the entire training dataset during the iterative re-weighting, are used to generate hard pseudo-labels. These weights, which range from 0 to 1, effectively capture the model’s converged confidence that a frame contains a stable, voiced signal. A hard pseudo-label $v_i^* \in \{0, 1\}$ is assigned by thresholding these final weights:

$$v_i^* = \begin{cases} 1 & \text{if } w_i > \theta \\ 0 & \text{otherwise} \end{cases}$$

where θ is a predefined confidence threshold. These pseudo-labels serve as the targets for the subsequent supervised training.

A lightweight, single-layer linear classification head is trained directly on the CQT spectrograms. This layer maps each CQT input frame X to a single logit for binary (voiced/unvoiced) classification. The classifier is optimized using standard binary cross-entropy loss against the generated pseudo-labels v^* . We deliberately choose a small, single-layer architecture over deeper multi-layer networks because the EM re-weighting process inherently down-weights some genuinely voiced frames during early iterations when F_0 estimates are still inaccurate. Larger models with greater capacity tend to overfit to these imperfect pseudo-labels, incorrectly learning to classify initially down-weighted but actually voiced frames as unvoiced. The limited capacity of a single linear layer provides natural regularization, forcing the classifier to capture only the most robust voicing patterns while generalizing better to frames that were temporarily misclassified during the iterative training process. While the feature extractor $f(\cdot)$ is not used for inference in this stage, its role in generating the high-quality pseudo-labels through the EM procedure is critical. This two-stage approach leverages the pitch structure learned during self-supervision to train a final, high-performance voicing detector without requiring any external ground-truth labels.

Harmonic Synthesizer

To qualitatively validate the accuracy of our predicted fundamental frequency (\hat{F}_0) and voicing (v) contours, we employ an analysis-by-synthesis procedure. We use a differentiable harmonic synthe-

sizer, illustrated in Figure 6, to reconstruct an audio segment using only the predicted \hat{F}_0 and v as inputs. The synthesizer’s parameters are then optimized to match the target audio, serving as a robust test of whether the predicted contours are sufficient for high-fidelity reconstruction.

Model Architecture The synthesizer is a specialized additive model that generates audio by summing H harmonics, where the amplitude of each harmonic is a learnable parameter that varies over time. The model’s inputs are the frame-wise \hat{F}_0 bin indices and the binary voicing flags v , both at the CQT frame rate (hop length of 160 samples).

1. **Input Pre-processing:** The \hat{F}_0 bin indices are first converted to Hertz using the CQT frequency lookup table. Both the \hat{F}_0 (Hz) contour and the voicing contour v are upsampled from the frame rate to the audio sample rate ($f_s = 16000$ Hz). We use linear interpolation for the \hat{F}_0 contour to ensure smooth frequency transitions and nearest-neighbor interpolation for the voicing contour to maintain sharp onsets and offsets. This results in sample-rate signals $f_0(t)$ and $v(t)$.
2. **Instantaneous Phase:** The instantaneous frequency for the h -th harmonic is $f_h(t) = h \cdot f_0(t)$. The instantaneous phase $\phi_h(t)$ is calculated by integrating the frequency, approximated as a cumulative sum of the phase increment, and adding a learnable per-harmonic global phase offset ψ_h :
$$\phi_h(t) = \left(2\pi \sum_{i=1}^t \frac{h \cdot f_0(i)}{f_s} \right) + \psi_h$$

where f_s is the sample rate (16000 Hz) and $\psi \in \mathbb{R}^H$ is a learnable parameter vector.
3. **Learnable Amplitude Envelopes:** The core of the synthesizer is its time-varying amplitude control. A learnable parameter matrix $G_{\text{pre}} \in \mathbb{R}^{H \times T}$ stores a pre-activation gain for each of the H harmonics at each of the T frames. These gains are passed through a Softplus function to ensure positivity, $G_f = \text{Softplus}(G_{\text{pre}})$, and are then linearly interpolated to the sample rate, yielding $g_h(t)$.
4. **Synthesis:** The final audio signal $s(t)$ is generated by summing the harmonics, each modulated by its specific gain envelope, the master voicing gate $v(t)$, and a learnable logarithmic master gain g_{master} . Harmonics with frequencies above the Nyquist limit ($f_s/2$) are masked

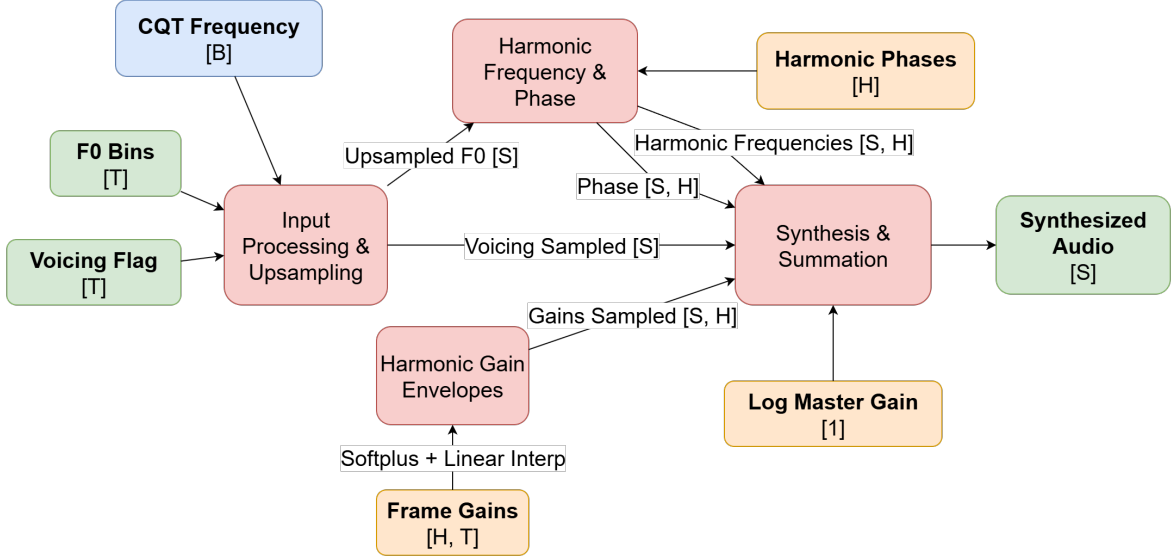


Figure 6: Harmonic Synthesizer Architecture for Analysis-by-Synthesis. Inputs (‘ F_0 Bins’, ‘Voicing Flag’) are processed and upsampled. Learnable parameters (‘Frame Gains’, ‘Harmonic Phases’, ‘Log Master Gain’) control harmonic frequencies, phases, and amplitudes. The synthesis stage combines these components, applying voicing and Nyquist masking, to generate the final audio output.

out.

$$s(t) = 10^{g_{\text{master}}} \cdot v(t) \cdot \sum_{h=1}^H g_h(t) \cdot \sin(\phi_h(t))$$

Optimization For a given target audio segment $y(t)$ and its corresponding \hat{F}_0 and v contours, we optimize the model’s learnable parameters: the frame-wise gains G_{pre} , the harmonic phases ψ , and the master gain g_{master} .

The objective is to minimize the perceptual difference between the synthesized audio $s(t)$ and the target $y(t)$. We use the Multi-Resolution STFT Loss (MR-STFT) from the auraloss library, which computes the L1 loss on the magnitudes and L2 loss on the log-magnitudes of the STFT across multiple resolutions (FFT sizes, hop sizes, and window sizes).

To encourage smooth and realistic amplitude envelopes, we add a smoothness regularizer. This penalty is the mean temporal Total Variation (TV) of the frame-wise gain matrix G_f , penalizing large, abrupt changes between adjacent frames:

$$\mathcal{L}_{\text{smooth}} = \frac{1}{H(T-1)} \sum_{h=1}^H \sum_{t=1}^{T-1} |G_f[h, t+1] - G_f[h, t]|$$

The final loss is a weighted sum:

$$\mathcal{L}_{\text{total}} = \mathcal{L}_{\text{MR-STFT}}(s, y) + \lambda \cdot \mathcal{L}_{\text{smooth}}$$

The model is trained for a fixed number of epochs using the Adam optimizer. This process effectively performs analysis-by-synthesis, finding the optimal harmonic amplitudes required to reconstruct the target audio given our model’s \hat{F}_0 and voicing predictions.